

ORIGINAL ARTICLE

The Diagnostic Performance of Magnetic Resonance Texture Analysis in Histological Subtyping and Grading of the Renal Cell Carcinoma

Renal Hücreli Karsinomun Histolojik Alt Tiplendirilmesi ve Derecelendirilmesinde Manyetik Rezonans Doku Analizinin Tanısal Performansı

¹Nusret Seher , ¹Mustafa Kolpay , ¹Abidin Kılincer , ²Lutfi Saltuk Demir , ³Mehmet Kaynar , ³Kadir Bocu ,
³Serdar Göktaş 

¹Department of Radiology, Faculty of Medicine, Selcuk University, Konya, Türkiye

²Department of Public Health, Faculty of Medicine, Necmettin Erbakan University, Konya, Türkiye

³Department of Urology, Faculty of Medicine, Selcuk University, Konya, Türkiye

Correspondence

Nusret Seher M.D.
Selcuk University, Medical Faculty,
Department of Radiology, The
Central Campus, 42075, Konya, Türkiye

E-Mail: nusretseher@gmail.com

How to cite ?

Seher N, Kolpay M, Kılincer A, Demir LS, Kaynar M, Bocu K, Göktaş S. The Diagnostic Performance of Magnetic Resonance Texture Analysis in Histological Subtyping and Grading of the Renal Cell Carcinoma. Genel Tıp Derg. 2025;35 (2): 255-263

ABSTRACT

Aim: Renal cell carcinoma (RCC) is the 6th most frequently diagnosed cancer worldwide in men and 10th in women, accounting for 5% of all oncological cases in men and 3% in women. RCC is usually detected incidentally but can be presented with symptoms such as lateral pain, hematuria, and a palpable mass. Therefore, we aimed to investigate and evaluate the efficiency of MRTA in distinguishing CC-RCC from NC-RCC, the three subtypes of RCC within each other, and high-grade and low-grade tumors.

Materials and Methods: Patients undergoing surgery for renal masses in our hospital between January 2015 and December 2019 and whose pathological diagnosis was RCC were determined and included in the study. Eighty-two patients with MR images in the Picture Archiving and Communication System (PACS) were retrospectively examined. The patient's age and gender were recorded. RCC subtypes and Fuhrman grades were determined according to histopathological results.

Results: Sixty-two patients were analyzed (34 males and 28 females). The average age of patients was 60.5 years (ranging between 24-81). Given the tumor localization, the tumors were located in the left kidney in 32 patients and the right kidney in 30 patients. Tumors were unilateral in all patients. Grouping according to RCC subtypes resulted in 40 CC-RCC (26 high-grade, 14 low-grade), 11 P-RCC (two high-grade, nine low-grade), and 11 CH-RCC.

Conclusion: MRTA revealed several parameters with satisfactory diagnostic performance in distinguishing CC-RCC from NC-RCC. Findings indicated that the texture analyses (TA) were the complements of the evaluation of multi-parametric magnetic resonance imaging (MRI) features. MRTA can be efficiently used as a noninvasive tool useful in subtyping and grading RCC. In routine practice, TA can be used in radiology departments as an adjunct modality to the findings of multiparametric MRI in patients with a preliminary diagnosis of RCC.

Keywords: Magnetic resonance texture analysis, renal cell carcinoma, tumor

ÖZ

Amaç: Renal hücreli karsinom (RCC), erkeklerde dünya çapında en sık teşhis edilen 6. ve kadınlarda 10. kanser olup, erkeklerde tüm onkolojik vakaların %5'ini ve kadınlarda %3'ünü oluşturmaktadır. RCC genellikle tesadüfen tespit edilir ancak lateral ağrı, hematuriya ve elle hissedilen kitle gibi semptomlarla ortaya çıkabilir. Bu nedenle, MRTA'nın CC-RCC'yi NC-RCC'den, RCC'nin üç alt tipini birbirini içinde ve yüksek dereceli ve düşük dereceli tümörleri ayırt etmedeki etkinliğini araştırmayı ve değerlendirmeyi amaçladık.

Materyaller ve Yöntemler: Ocak 2015 ile Aralık 2019 arasında hastanemizde renal kitle nedeniyle ameliyat edilen ve patolojik tanısı RCC olan hastalar belirlendi ve çalışmaya dahil edildi. Resim Arşivleme ve İletişim Sisteminde (PACS) MR görüntüleri olan 82 hasta retrospektif olarak incelendi. Hastanın yaşı ve cinsiyeti kaydedildi. RCC alt tipleri ve Fuhrman dereceleri histopatolojik sonuçlara göre belirlendi.

Bulgular: Altmış iki hasta analiz edildi (34 erkek ve 28 kadın). Hastaların ortalama yaşı 60,5 yıldır (24-81 arasında değişiyordu). Tümör lokalizasyonuna bakıldığında, tümörler 32 hastada sol böbrekte ve 30 hastada sağ böbrekte yer alıyordu. Tümörler tüm hastalarda tek taraflıydı. RCC alt tiplerine göre gruplandırma sonucunda 40 CC-RCC (26 yüksek dereceli, 14 düşük dereceli), 11 P-RCC (iki yüksek dereceli, dokuz düşük dereceli) ve 11 CH-RCC ortaya çıktı.

Sonuç: MRTA, CC-RCC'yi NC-RCC'den ayırt etmede tatmin edici tanı performansına sahip birkaç parametre ortaya koydu. Bulgular, doku analizlerinin (TA) çok parametrelili manyetik rezonans görüntüleme (MRI) özelliklerinin değerlendirilmesinin tamamlayıcısı olduğunu gösterdi. MRTA, RCC'nin alt tiplendirilmesi ve derecelendirilmesinde yararlı olan invaziv olmayan bir araç olarak etkili bir şekilde kullanılabilir. Rutin uygulamada, TA, RCC ön tanısı olan hastalarda multiparametrik MRI bulgularına ek bir modalite olarak radyoloji bölümlerinde kullanılabilir.

Anahtar kelimeler: Manyetik rezonans doku analizi, renal hücreli karsinom, tümör

Introduction

Worldwide, renal cell carcinoma (RCC) is the 6th most frequently diagnosed cancer in men and 10th diagnosed in women, accounting for 5% of all oncological cases in men and 3% in women(1, 2). Although it is usually detected incidentally, it can be presented with symptoms such as lateral pain,

hematuria, and a palpable mass. Approximately 17% of patients with RCC have metastases at the time of diagnosis(3). Early diagnosis of RCC is important since it is a tumor that is generally detected incidentally and has nonspecific symptoms. More than 90% of RCC consist of three main sub-types (clear cell RCC

(CC-RCC) 75-80%, papillary RCC (P-RCC) 5-10%, and chromophobe RCC (CH-RCC) 5-10%). The histological subtype is one of the important prognostic factors. CC-RCC has higher mortality than non-clear (NC)-RCC(4, 5). The most important prognostic factor is the nuclear grading of the TNM stage and Fuhrman, consisting of four degrees (low-grade: 1 and 2; high-grade: 3 and 4) based on nuclear morphology and pleomorphism(6-9). Clear cell RCCs are more metastatic and mortal tumors, and it is estimated that 70%-90% of them show changes in the von Hippel-Landau gene by mutation or gene silencing (i.e. hypermethylation)(10, 11). Preoperative diagnosis is important for CC-RCC. Tyrosine kinase inhibitors such as sunitinib and mammalian target of rapamycin (mTOR) inhibitors such as everolimus are used for successful surgery in CC-RCCs (70-90% VHL gene mutation is present) as they decrease micrometastasis and increase surgical success (4). Therefore, the prognosis varies depending on anatomical, clinical, histological, and molecular factors. Thus, preoperative estimation of tumor subtype and grade is needed, and it can be done through the use of noninvasive tools such as imaging. Although rapid development in computed tomography (CT) and magnetic resonance imaging (MRI) has recently provided insight into anatomical and prognostic factors, it cannot provide sufficient data on the histological types of RCC and tumor behavior(12-15).

Texture analysis (TA) evaluates tumor heterogeneity at the pixel level through the distribution and spatial relationship of grayscale values and identifies the presence of small differences, potentially not perceptible to the human eye. It reflects areas such as tumor heterogeneity, necrosis, high cell density, and bleeding. Heterogeneity is also a known feature of malignancy as an essential prognostic factor because it is thought that high tumor heterogeneity may be associated with high tumor levels(16). Many studies have used TA for subtyping and grading RCC in contrast to enhanced CT images(17-22). In this study, we investigated MR texture analysis (MRTA) as a tool for subtyping and grading RCC. MRI provides multiple paradigms for the evaluation of morphology. Therefore, MRTA is more likely to provide more robust data than CT. This study aims to investigate and evaluate the efficiency of MRTA in distinguishing CC-RCC from NC-RCC, the three subtypes of RCC within each other, and high-grade and low-grade tumors.

Materials And Methods

Patient Selection

Following receipt of the ethics committee number 2020/189 from our university ethics committee, patients who underwent surgery for renal masses in our hospital between January 2015 and December 2019 and whose

pathological diagnosis was RCC were determined. The study was conducted under the principles of the Declaration of Helsinki. 82 patients with MR images in the Picture Archiving and Communication System (PACS) were retrospectively examined. The age and gender of the patients were recorded. RCC subtypes and Fuhrman grades were determined according to histopathological results. Pathologically, tumors without uniform subtypes, tumors with sarcomatous features, tumors with rhabdoid features, and tumors without Fuhrman grading were excluded from the study. Patients with artifacts on MRI and non-optimal (such as the corticomedullary phase or nephrogram phase not being in the expected contrast staining phase) corticomedullary (CM) and nephrographic (NG) phases taken after the contrast were excluded from the study. Finally, a total of 62 RCC patients were analyzed.

The Magnetic Resonance Imaging (MRI) Protocol

All the MRI examinations were performed on a 1.5-T scanner (Aera, Siemens, Erlangen, Germany). From the pre-contrast sequences, axial T2-weighted (W) Half-Fourier Acquisition Single-shot Turbo Spin Echo (HASTE), axial T1W dual gradient echo in-phase (IP) and apparent diffusion coefficient (ADC) images were used. In the series taken after the contrast, images obtained in the CM (35-40 sec) and NG (90-100 sec) phases of the axial fat-saturated T1W Volume Interpolated Breath-hold Examination (VIBE) sequence were used. The use of contrast material included Gadovist (Bayer HealthCare) infusion at a dose of 0.1 mmol/kg followed by a 25 ml saline flush (administered at a rate of 3 mL /s using a power injector).

The Texture Analysis

Texture analysis was performed on 62 patients whose images were available. One radiologist with five years of experience in diagnostic imaging performed the texture analysis and he was blinded to the final histopathological diagnosis. For the analysis, axial T2W (Half Fourier Single-shot Turbo spin-Echo) HASTE images, axial T1W dual gradient echo IP images, ADC map, and the post-contrast (CM and NG phase) axial T1-VIBE images were used. The images were sent to the database of the TA program. MRTA was performed using software (Olea Medical, a Canon Group Company, Japan) by placing the freehand region of interest (ROI) in tumors to contain the entire tumor in all sequences. Axial T2W HASTE images were scanned to map the distribution of the tumor component that was initially traceable. Then, all the sequences to be measured were stacked side by side in the TA program, the only representative slice showing the entire tumor component was selected, and the ROI was plotted to cover almost all of the tumor in any sequence (Figure 1a-e).

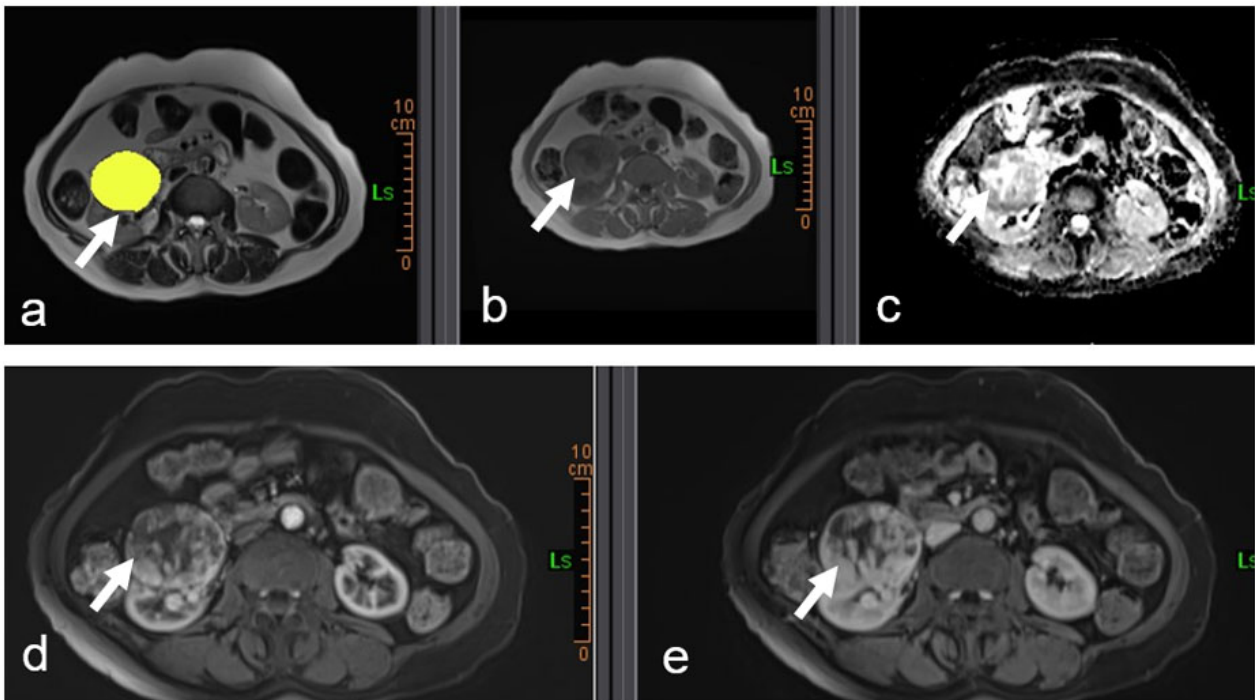


Figure 1. The sequences to be used in texture analysis were arranged side by side with the same sections (T2W (a), IP(b), ADC(c), CM phase(d), and NG phase (e)). Then, the ROI was drawn on one of the sequences to take up the entire tumor (arrow).

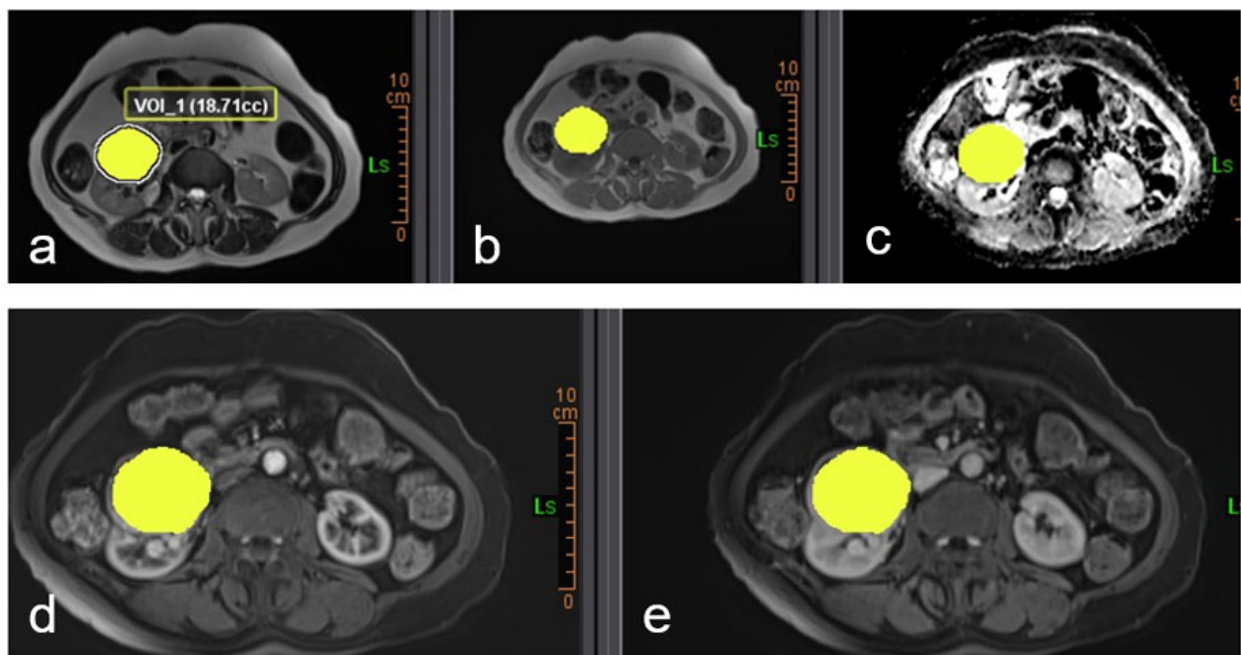


Figure 2. The ROI drawn on one of the sequences was copied to all sequences, in the same way, to avoid irregularities in the measurements (T2W (a), IP (b), ADC (c), CM phase (d), and NG phase (e)).

The ROI was then copied from the drawn sequence to other sequences (Figure 2a-e). Care was taken not to extend the ROI limits to peripheral 1-2 mm of the tumor to avoid possible errors. In tumors with a cystic or necrotic component weight, the ROI was plotted to include the solid part. After the ROIs were placed

in the sequences, TA was performed in the Olea TA program using 7 separate parameters for each sequence. One of the most significant advantages of the Olea TA program was that it showed the analysis results in seconds (Figure 3). Parameters used for the TA included mean (average of the gray level intensity),

Features	ep2d_diff_FS_b50_400_800_p2_ADC_...	t1_fl2d_opp-in_t...	t1_vibe_fs_tra...	t1_vibe_fs_tra...	t2_haste_tra...
	VOI_3#1	VOI_2#1	VOI_4#1	VOI_5#1	VOI_1#1
Original First Order					
Entropy	5.560	4.783	5.527	5.595	5.429
Mean	1878.504	143.513	218.184	274.582	501.852
Median	1843.000	144.000	221.000	290.000	490.000
Skewness	0.082	-0.505	-0.027	-0.631	0.281
Kurtosis	2.457	5.252	2.216	2.714	2.631
Variance	83210.822	132.569	9130.391	8220.091	12380.816
Uniformity	0.024	0.042	0.024	0.024	0.027

Figure 3. Following the ROI drawing and selection of statistical parameters, a texture analysis results screen is shown.

median (value separating the higher half gray levels intensities within the ROI, from the lower half), entropy (the average amount of information required to encode the image values), skewness (asymmetry of the distribution of values about the mean value), kurtosis (peakedness of the histogram), variance (squared distances of each intensity value from the Mean value), uniformity (sum of the squares of each intensity value). Thus, 35 different measurements were made with 5 sequences and 7 different parameters for each patient.

Statistical Analysis

Statistical analysis was done using SPSS software (IBM Corp, Armonk, NY, USA) for Windows. The Kolmogorov-Smirnov test was used to determine the normal distribution of continuous variables. Quantitative variables were expressed as median with range (min □ max) since the MRTA parameters were not distributed normally. Comparisons between the groups were performed using Kruskal-Wallis or Mann-Whitney's U test for quantitative variables, as appropriate. A P value of <0.05 was considered significant. Then, the

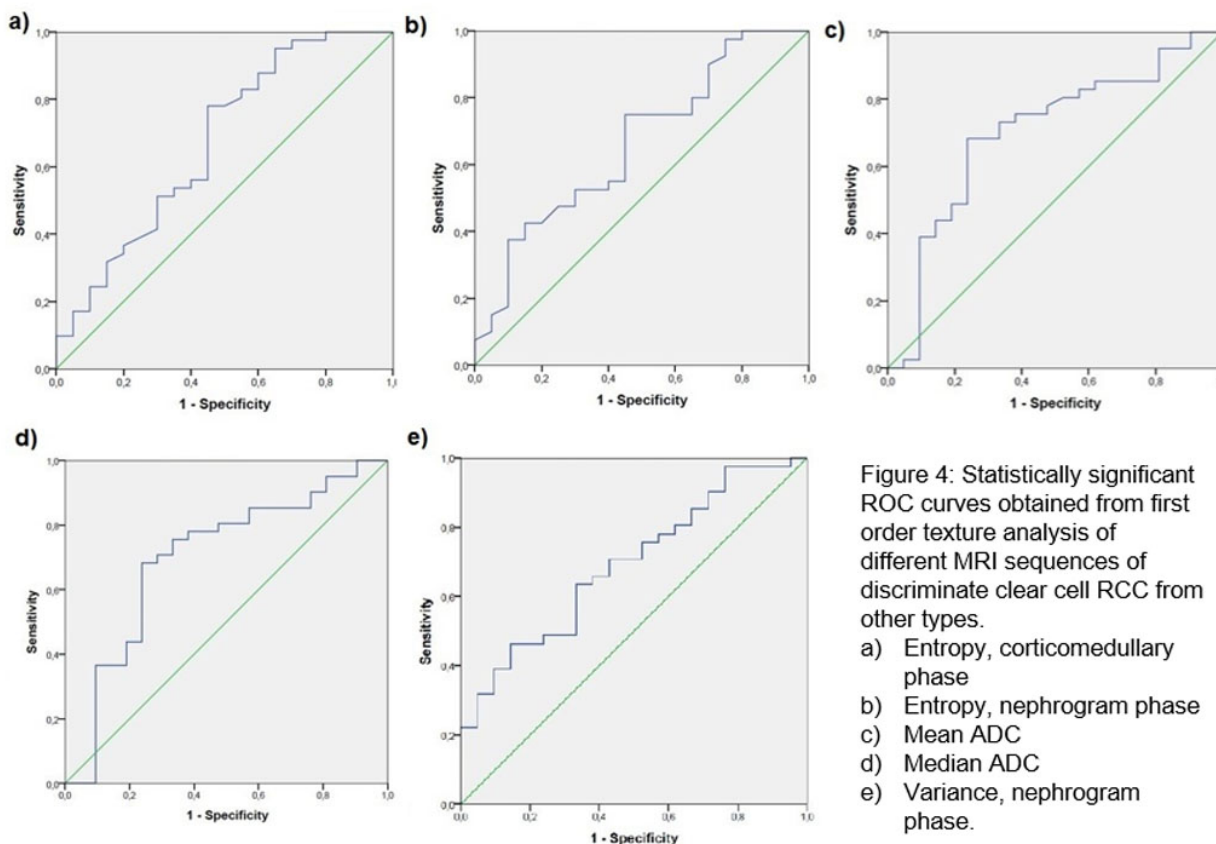


Figure 4: Statistically significant ROC curves obtained from first order texture analysis of different MRI sequences of discriminate clear cell RCC from other types. a) Entropy, corticomedullary phase b) Entropy, nephrogram phase c) Mean ADC d) Median ADC, e) Variance, nephrogram phase.

Figure 4. Statistically significant ROC curves obtained from first-order texture analysis of different MRI sequences of discriminate clear cell RCC from other types. a) Entropy, corticomedullary phase b) Entropy, nephrogram phase c) Mean ADC, d) Median ADC, e) Variance, nephrogram phase.

Receiver Operating Characteristic (ROC) analysis was performed on those with a significant P value in the data obtained. The area under the curve (AUC), cut-off values, sensitivity, and specificity values were determined.

Results

Sixty-two patients were analyzed (34 male, 28 female). The average age of patients was 60.5 (range, 24-81). When the tumor localization was examined, the tumor was located in the left kidney in 32 patients and the right kidney in 30 patients. Tumors were unilateral in all patients. Grouping according to RCC subtypes resulted in 40 CC-RCC (26 high-grade, 14 low-grade), 11 P-RCC (two high-grade, nine low-grade), and 11 CH-RCC.

Differentiation of CC-RCC from NC-RCC

After the Mann-Whitney U analysis was done, the P values of the 7 parameters used were calculated individually for each MR sequence and are shown in Table 1. In the statistical analysis, there were significant values in the differentiation of CC-RCC from NC-RCC in ADC, CM phase, and NG phase. In IP and T2W images, it was observed that the parameters used were not significant in distinguishing CC-RCC from NC-RCC. NG phase was observed to be the most significant sequence in distinguishing CC-RCC and NC-RCC. Significant values in the ROC analysis are shown in Table 2 and Figure 4.

Table 1. Mann-Whitney U test in distinguishing CC-RCC from NC-RCC

Sequences	Parameters	CC-RCC (n=40)	NC-RCC (n=22)	P (Mann-Whitney U) CC-NC RCC
ADC	Mean	1515 (649-2672)	1193 (271-2934)	0.011*
	Median	1528 (626-2714)	1166 (209-2933)	0.01*
	Skewness	-0.198 (-1.71-3.04)	0.34 (-1.36-2.28)	0.022*
	Kurtosis	3.77 (0.63-15.8)	3.72 (1.10-9.71)	0.87
	Variance	132400 (1562-980895)	63031 (6931-433098)	0.026*
	Uniformity	0.035 (0.02-0.17)	0.037 (0.02-0.10)	0.36
	Entropy	5.1 (3.78-5.64)	5.04 (4.06-5.57)	0.38
IP	Mean	188 (160-2705)	186(106-306)	0.17
	Median	185 (79-329)	175 (107-321)	0.19
	Skewness	0.55 (-1.87-2.88)	0.44 (-0.92-3.87)	0.25
	Kurtosis	4.7 (2.04-18.07)	3.27 (2.24-25.12)	0.09
	Variance	509 (65-9623)	461 (99-9319)	0.79
	Entropy	5.04 (4.07-5.68)	5.16 (3.97-5.53)	0.15

Corti-come-dullar phase	Mean	152 (54-604)	139 (80-685)	0.42
	Median	219 (51-626)	133(75-684)	0.48
	Skewness	0.1 (-42-.96)	-0.057 (-1.79-8.38)	0.48
	Kurtosis	3.24 (1.74-10.88)	4.30 (1.99-30.26)	0.017*
	Variance	2312 (224-35062)	1271 (82-8794)	0.066*
	Uniformity	0.032 (0.02-0.05)	0.037 (0.02-0.10)	0.009*
	Entropy	5.3 (4.72-5.70)	5.07 (3.76-5.58)	0.017*
Neph-rogram phase	Mean	222 (65-526)	191 (104-333)	0.1
	Median	227 (64-551)	183 (88-354)	0.049*
	Skewness	-0.55 (-4.12-1.74)	0.12 (-2.01-3.58)	0.065
	Kurtosis	3.19 (0.48-8.95)	4.32 (2.28-23.41)	0.018*
	Variance	2975 (134-24368)	1876 (131-6401)	0.014*
	Uniformity	0.035 (0.02-0.06)	0.04 (0.03-0.09)	0.026*
	Entropy	5.27 (4.6-6.7)	4.95 (3.96-5.54)	0.017*
T2W	Mean	188 (105-604)	312 (148-845)	0.33
	Median	339 (156-596)	304 (144-851)	0.34
	Skewness	0.34 (-0.97-2.28)	0.34 (-0.97-2.28)	0.59
	Kurtosis	3.37 (1.58-16.5)	3.54 (1.69-9.62)	0.57
	Variance	4967 (180-32947)	2427 (370-47086)	0.36
	Uniformity	0.034 (0.02-0.07)	0.036 (0.02-0.07)	0.28
	Entropy	5.15 (4.17-5.71)	4.99 (4.27-5.62)	0.1

Median (Min-Max). Significant p-values are indicated with*. ADC: Apparent diffusion coefficient, CM: Corticomedullary, IP: In-phase, NG: Nephrogram, T2W: T2-weighted.

Table 2. Diagnostic performance of parameters and AUC values that are statistically significant.

Sequences	Parameters	AUC	Cut-off Value	Sensitivity	Specificity
ADC	Mean	0.75	1181	80	50
ADC	Median	0.76	1192.25	80.5	66.7
CM Phase	Entropy	0.67	5.01	82.9	45
NG Phase	Entropy	0.66	4.95	75	55
NG Phase	Variance	0.66	826.5	83.8	33.3

ADC: Apparent diffusion coefficient, AUC: Area under the curve, CM: Corticomedullary, NG: Nephrogram

Differentiation of Subtypes

A non-parametric Kruskal Wallis test was completed to compare the differences in texture parameters between the subtypes. The measured p values are shown in detail in Table 3. Non-parametric Mann-Whitney U test was used for the binary distinction of the subtypes. In separating CC-RCC from P-RCC; In the ADC sequence, the mean was significantly higher than P-RCC in CC-RCC (p=0.024). Median was significantly higher in CC-RCC than P-RCC (p=0.021). In the CM phase, uniformity was significantly lower in CC-RCC than in P-RCC (p = 0.048). In the NG phase, kurtosis was significantly lower than P-RCC in CC-RCC (p=0.048). Uniformity was significantly lower in CC-RCC than in P-RCC (p=0.003). In distinguishing CC-RCC from CH-RCC; and in the ADC sequence, the variance was significantly higher in CC-RCC than CH-RCC (p=0.03).

In the distinction between P-RCC and CH-RCC; in the NG phase, kurtosis was significantly higher than CH-RCC in P-RCC ($p=0.021$). Uniformity was significantly higher in P-RCC than in CH-RCC ($p=0.024$). There was no significant difference in parameters measured in IP and T2W sequences.

Table 3. Kruskal Wallis test in differentiating RCC subtypes

Sequences	Parameters	CC-RCC (n=40)	P-RCC (n=11)	CH-RCC (n=11)	P (Kruskal-Wallis)
ADC	Mean	1515 (649-2672)	1084 (271-2628)	1294 (703-2934)	0.019*
	Median	1528 (626-2714)	1046 (209-2771)	1240 (693-2933)	0.016*
	Skewness	-0.198 (-1.71-3.04)	0.34 (-1.36-2.28)	0.39 (-0.33-1.65)	0.067
	Kurtosis	3.77 (.63-15.8)	3.53 (2.30-9.71)	3.83 (1.10-6.99)	0.97
	Variance	132400 (1562-980895)	70813 (17412-433098)	34313 (6931-197276)	0.031*
	Uniformity	0.035 (0.02-0.17)	0.034 (0.02-0.10)	0.039 (0.03-0.07)	0.58
	Entropy	5.1 (3.78-5.64)	5.11 (4.38-5.57)	4.98 (4.06-5.31)	0.55
IP	Mean	188 (160-2705)	189 (106-306)	177 (126-286)	0.27
	Median	185 (79-329)	173 (107-321)	178 (125-281)	0.35
	Skewness	0.55 (-1.87-2.88)	0.43 (-0.92-0.90)	0.44 (-0.78-3.87)	0.44
	Kurtosis	4.7 (2.04-18.07)	3.15 (2.38-9.05)	3.62 (2.24-25.12)	0.22
	Variance	509 (65-9623)	1179 (246-9319)	240 (99-4764)	0.088
	Uniformity	0.039 (0.03-0.07)	0.037 (0.03-0.07)	0.036 (0.03-0.09)	0.637
CM Phase	Entropy	5.04 (4.07-5.68)	5.15 (4.33-5.53)	5.18 (3.97-5.49)	0.31
	Mean	152 (54-604)	139 (84-273)	145 (80-685)	0.61
	Median	219 (51-626)	126 (75-289)	147 (77-684)	0.55
	Skewness	0.1 (-0.42-0.96)	0.17 (-1.79-0.63)	-0.19 (-1.73-8.38)	0.68
	Kurtosis	3.241 (0.74-10.88)	4.3 (1.99-8.67)	3.88 (2.89-30.26)	0.056
	Variance	2312 (224-35062)	2357 (239-8794)	630 (82-5981)	0.13
	Uniformity	0.032 (0.02-0.05)	0.039 (0.03-0.06)	0.035 (0.02-0.10)	0.033*
Entropy	5.3 (4.72-5.70)	5.02 (4.61-5.58)	5.14 (3.76-5.54)	0.057	

NG Phase	Mean	222 (65-526)	191 (104-333)	188 (105-280)	0.26
	Median	227(64-551)	190 (88-354)	183 (109-287)	0.13
	Skewness	-0.55 (-4.12-1.74)	0.21 (-1.96-3.58)	-0.07 (-2.01-3.12)	0.17
	Kurtosis	3.19 (.48-8.95)	6.66 (3.02-23.41)	3.22 (2.28-9.20)	0.003*
	Variance	2975 (134-24368)	1876 (292-6401)	1834 (131-4712)	0.048*
	Uniformity	0.035 (0.02-0.06)	0.049 (0.03-0.09)	0.031 (0.03-0.06)	0.003*
	Entropy	5.27 (4.6-6.7)	4.83 (3.96-5.40)	5.24 (4.64-5.54)	0.004*
T2W	Mean	188 (105-604)	292 (148-845)	354 (172-810)	0.27
	Median	339 (156-596)	274 (144-851)	351 (173-839)	0.21
	Skewness	0.34 (-0.97-2.28)	0.58 (0.15-2.23)	0.41 (-1.55-1.02)	0.42
	Kurtosis	3.37 (1.58-16.5)	3.74 (1.69-9.62)	3.54 (2.33-5.22)	0.83
	Variance	4967 (180-32947)	3177 (1073-47086)	2272 (370-44705)	0.51
	Uniformity	0.034 (0.02-0.07)	0.038 (0.03-0.07)	0.035 (0.02-0.04)	0.38
	Entropy	5.15 (4.17-5.71)	4.88 (4.27-5.46)	5.12 (4.88-5.62)	0.13

Median (Min-Max). Significant p-values are indicated with*. ADC: Apparent diffusion coefficient, CM: Corticomedullary, IP: In-phase, NG: Nephrogram, T2W: T2-weighted

Differentiation of Histologic Grade

A Mann-Whitney U test was completed to compare the differences in texture parameters between low-grade (1,2) and high-grade (3,4). In the IP sequence, the variance was significantly higher in the group with a low histologic grade than in the group with a high grade ($p=0.024$). In T2W images, the variance was significantly higher in the group with a low histologic grade than in the group with a high grade ($p=0.0037$). There was no significant difference in parameters measured in other sequences.

Discussion

Renal cell carcinoma is ranked as the 13th most common cause of death from cancer worldwide. More importantly, although most of the lesions detected are small in size, the locally advanced disease is present in a significant proportion of patients. In some patients, distant metastases can be seen at the time of diagnosis(2). The locally advanced disease, micrometastasis, and lymph node metastasis are more evident in CC-RCC(4, 5). Due to such situations, early diagnosis is vital in RCC. As known, the gold standard method is histopathological evaluation. Patients suspected of RCC may have a biopsy for early diagnosis and treatment, to determine the subtype and Fuhrman grade. However, a biopsy is an invasive procedure, and the sample tissue piece needs to contain a sufficient amount of tumoral tissue. Histological staging of RCC can be performed in

percutaneous biopsy, but it is generally not considered correct due to sampling problems, and the majority of tumors vary in histological grade compared to biopsy after nephrectomy(23). Also, the most important complications that can occur in a biopsy include the risk of bleeding (3.5%) and, most importantly, the risk of tumor seeding to the biopsy tract(24). So, the importance of the noninvasive diagnosis is gradually increasing. In the radiology literature, it is seen that the articles on noninvasive diagnosis of RCC have increased rapidly in recent years. In many of these articles, contrast enhancement patterns of tumors were emphasized with CT and MRI, subtype distinction, low-high-grade separation, and inferences were made more quantitatively(25-28). Vargas et al., in their multiparametric MRI study, showed that the percentage of signal intensity (SI) change in sequences taken after contrast in the distinction between subtypes could distinguish CC-RCC from other subtypes(27). To this date, there is ongoing research for noninvasive imaging techniques that can provide preoperative prognostic information for tumor subtype and grade and reduce the need for biopsy. TA articles related to RCC are limited in the literature. Many studies achieved satisfactory diagnostic performance in grading and subtyping RCC in contrast to enhanced CT images using the TA program(17-22).

Our study is an MRTA study with the largest patient population with RCC subtypes. In this study, we examined the performance of MRTA in three ways. First, we examined the performance of distinguishing CC-RCC from NC-RCC, second in distinguishing 3 subtypes between each other, and thirdly, differentiating low-grade (1-2) and high-grade (3-4) tumors according to the Fuhrman classification. MRI provides several advantages due to its high temporal resolution in the morphological and functional evaluation of tumors (T1W, T2W, post-contrast images, DWI), and the evaluation of their relationship with surrounding tissues. Therefore, it is more likely that MRTA can provide more robust and reliable data compared to the CT texture analysis. There are two MRTA studies on RCC in the literature. Vendrami et al. tried to distinguish two subtypes of P-RCC and showed that the combination of qualitative analysis and TA improves the prediction of type 2 tumors(2). Goyal et al., in a study of 34 patients, found significant results in distinguishing CC-RCC from NC-RCC with various texture parameters and in separating high-grade and low-grade CC-RCC(29). Our study showed a strong diagnostic performance in MRTA in the distinction of CC-RCC and NC-RCC with various texture parameters. Additionally, we obtained significant results in MRTA for distinguishing RCC subtypes and low-high-grade tumors.

Texture analysis measures heterogeneity by evaluating the background signal intensity and brightness

differences according to the parameters used. Entropy and variance, dispersion and irregularity measurement tend to be higher at higher degrees of heterogeneity. Kurtosis, which is a measure of the histogram's peak, decreases with more heterogeneity. Mean and median, on the other hand, are associated with overall brightness, showing a positive correlation with higher signal intensity and amplification(16-20). Skewness defines the asymmetry of the mean value and shifts the tail of the histogram to the right (positive skewness) or left (negative skewness) depending on the increase and decrease in the number of bright pixels. Uniformity increases depending on the heterogeneity in the environment.

CC-RCC is more heterogeneous due to more necrosis than NC-RCC in terms of imaging properties, and CC-RCC is also more contrasted than P-RCC(18). In our study, according to the data, entropy, variance, and uniformity values were significantly higher in CC-RCC due to heterogeneity, especially in measurements performed in the post-contrast CM and NG phase.

In the literature, it was shown that P-RCC has more homogeneous diffusion restriction while CC-RCC has more heterogeneous diffusion restriction(25). In our study, when the parameters used in ADC were examined, the mean, median, and variance parameters were significantly higher in CC-RCC than in NC-RCC. Based on these values, it is understood that CC-RCC has a more heterogeneous ADC map.

When the low and high-grade tumors were compared, high-grade tumors were expected to show stronger contrast uptake and greater diffusion constraint. This suggests that ADC should show more positive skewness, and entropy in CM and NG phases. However, Cornelis et al. stated that the correlation of ADC and contrasted images with tumor grade remained weak(26). In our study, in the IP and T2W sequences, the variance parameter was significantly higher in low-grade tumors. These results caused us to think that as the tumor grade increases, the rate of microscopic and macroscopic fat decreases while necrosis increases. So, the standard deviation (SD) was higher since the fat component was more in lower grades; accordingly, the variance was significantly higher.

In the comparison of subtypes, the mean and median parameters in ADC were significantly higher in CC-RCC when compared with P-RCC, which showed that CC-RCC restricted more heterogeneous diffusion than expected. CC-RCC has a more heterogeneous pattern while P-RCC has a more homogeneous contrast pattern(27). Accordingly, in the CM and NG phases, uniformity was higher in P-RCC, while kurtosis in the NG phase was significantly lower in CC-RCC. In the comparison of CC-RCC and CH-RCC, the variance

in ADC was significantly higher in CC-RCC, which supported that CC-RCC is a more heterogeneous tumor. In the P-RCC/CH-RCC distinction, kurtosis and uniformity in the NG phase were higher in P-RCC than in CH-RCC, which indicates that P-RCC is contrasted less in the NG phase and more homogenous compared to CH-RCC(26).

Our study has yielded several texture parameters that perform well in differentiating CC-RCC from NC-RCC and high-grade low-grade CC-RCC and distinguishing subtypes from each other. TA has become an important topic that has been the focus of an increasing number of publications over the past decade. Tumor heterogeneity is an important prognostic factor, as well as one of the known essential features of malignancy because higher tumor heterogeneity is thought to be associated with higher tumor grades. TA uses a variety of mathematical methods that can be used to assess the gray level intensity and position of pixels in the image to extract texture features that can predict intralesional heterogeneity(28). In light of this information, TA is emerging as an essential tool in oncological imaging. However, in the future, if definitive evidence can be obtained, it can be used as a quantitative tool to assist in the morphological evaluation of renal tumors.

Our study had some limitations. First, our low-grade tumor count was lower than the high-grade tumor count. Second, we evaluated only the first order as statistical texture parameters. Advanced-level statistical parameters can provide more data size. Studies of the most advanced-level statistical parameters are not available in the literature, and the biological basis of these parameters is not yet known. Our study is a single-center study; multicenter studies for the diagnosis of RCC are also needed to support our findings.

In conclusion, the MRTA showed several parameters with satisfactory diagnostic performance (AUC > 0.75) in distinguishing CC-RCC from NC-RCC. Findings show that the TA complements the evaluation of multiparametric MRI features. MRTA can be efficiently used as a noninvasive tool useful in subtyping and grading RCC. In routine practice, TA can be used in radiology centers as an adjunct to the findings of multiparametric MRI in patients with a preliminary diagnosis of RCC.

Conflict of Interest

The authors declare that they have no conflict of interest.

Financial Support

This study has received no funding.

References

1.Siegel RL, Miller KD, Jemal A. Cancer Statistics, 2018. CA

Cancer J Clin. 2018 Jan;68(1):7-30.

2.Capitanio U, Montorsi F. Renal Cancer. Lancet. 2016 Feb 27;387(10021):894-906.

3.Capitanio U, Bensalah K, Bex A, et al. Epidemiology of Renal Cell Carcinoma. Eur Urol. 2019 Jan;75(1):74-84.

4.Posadas EM, Limvorasak S, Figlin RA. Targeted Therapies for Renal Cell Carcinoma. Nat Rev Nephrol. 2017 Aug;13(8):496-511.

5.Shao Y, Xiong S, Sun G, et al. Prognostic Analysis of Postoperative Clinically Nonmetastatic Renal Cell Carcinoma. Cancer Med. 2020 Feb;9(3):959-970.

6.Ficarra V, Galfano A, Novara G, et al. Risk Stratification and Prognostication of Renal Cell Carcinoma. World J Urol. 2008 Apr;26(2):115-125.

7.Muglia VF, Prando A. Renal Cell Carcinoma: Histological Classification and Correlation with Imaging Findings. Radiol Bras. 2015 May-Jun;48(3):166-174.

8.Volpe A, Patard JJ. Prognostic Factors in Renal Cell Carcinoma. World J Urol. 2010 Jun;28(3):319-327.

9.Escudier B, Porta C, Schmidinger M, et al. Renal Cell Carcinoma: Esmo Clinical Practice Guidelines for Diagnosis, Treatment and Follow-Up. Ann Oncol. 2016 Sep;27(suppl 5):v58-v68.

10.Moore LE, Nickerson ML, Brennan P, et al. Von Hippel-Lindau (Vhl) Inactivation in Sporadic Clear Cell Renal Cancer: Associations with Germline Vhl Polymorphisms and Etiologic Risk Factors. PLoS Genet. 2011 Oct;7(10):e1002312.

11.Sudarshan S, Karam JA, Brugarolas J, et al. Metabolism of Kidney Cancer: From the Lab to Clinical Practice. Eur Urol. 2013 Feb;63(2):244-251.

12.Kim JH, Bae JH, Lee KW, Kim ME, Park SJ, Park JY. Predicting the Histology of Small Renal Masses Using Preoperative Dynamic Contrast-Enhanced Magnetic Resonance Imaging. Urology. 2012 Oct;80(4):872-876.

13.Jung SC, Cho JY, Kim SH. Subtype Differentiation of Small Renal Cell Carcinomas on Three-Phase MdcT: Usefulness of the Measurement of Degree and Heterogeneity of Enhancement. Acta Radiol. 2012 Feb 1;53(1):112-118.

14.Young JR, Margolis D, Sauk S, Pantuck AJ, Sayre J, Raman SS. Clear Cell Renal Cell Carcinoma: Discrimination from Other Renal Cell Carcinoma Subtypes and Oncocytoma at Multiphasic Multidetector Ct. Radiology. 2013 May;267(2):444-453.

15.Sasaguri K, Takahashi N. Ct and Mr Imaging for Solid Renal Mass Characterization. Eur J Radiol. 2018 Feb;99:40-54.

16.Hodgdon T, McInnes MD, Schieda N, Flood TA, Lamb L, Thornhill RE. Can Quantitative Ct Texture Analysis Be Used to Differentiate Fat-Poor Renal Angiomyolipoma from Renal Cell Carcinoma on Unenhanced Ct Images? Radiology. 2015 Sep;276(3):787-796.

- 17.Lubner MG, Stabo N, Abel EJ, Del Rio AM, Pickhardt PJ. Ct Textural Analysis of Large Primary Renal Cell Carcinomas: Pretreatment Tumor Heterogeneity Correlates with Histologic Findings and Clinical Outcomes. *AJR Am J Roentgenol.* 2016 Jul;207(1):96-105.
- 18.Yu H, Scalera J, Khalid M, et al. Texture Analysis as a Radiomic Marker for Differentiating Renal Tumors. *Abdom Radiol (NY).* 2017 Oct;42(10):2470-2478.
- 19.Zhang GM, Shi B, Xue HD, Ganeshan B, Sun H, Jin ZY. Can Quantitative Ct Texture Analysis Be Used to Differentiate Subtypes of Renal Cell Carcinoma? *Clin Radiol.* 2019 Apr;74(4):287-294.
- 20.Bektas CT, Kocak B, Yardimci AH, et al. Clear Cell Renal Cell Carcinoma: Machine Learning-Based Quantitative Computed Tomography Texture Analysis for Prediction of Fuhrman Nuclear Grade. *Eur Radiol.* 2019 Mar;29(3):1153-1163.
- 21.Shu J, Tang Y, Cui J, et al. Clear Cell Renal Cell Carcinoma: Ct-Based Radiomics Features for the Prediction of Fuhrman Grade. *Eur J Radiol.* 2018 Dec;109:8-12.
- 22.Yaşar S, Voyvoda N, Voyvoda B, Özer T. Using Texture Analysis as a Predictive Factor of Subtype, Grade and Stage of Renal Cell Carcinoma. *Abdom Radiol (NY).* 2020 Nov;45(11):3821-3830.
- 23.Schieda N, Lim RS, Krishna S, McInnes MDF, Flood TA, Thornhill RE. Diagnostic Accuracy of Unenhanced Ct Analysis to Differentiate Low-Grade from High-Grade Chromophobe Renal Cell Carcinoma. *AJR Am J Roentgenol.* 2018 May;210(5):1079-1087.
- 24.Andersen MF, Norus TP. Tumor Seeding with Renal Cell Carcinoma after Renal Biopsy. *Urol Case Rep.* 2016 Nov;9:43-44.
- 25.Schieda N, Lim RS, McInnes MDF, et al. Characterization of Small (<4cm) Solid Renal Masses by Computed Tomography and Magnetic Resonance Imaging: Current Evidence and Further Development. *Diagn Interv Imaging.* 2018 Jul-Aug;99(7-8):443-455.
- 26.Cornelis F, Tricaud E, Lasserre AS, et al. Routinely Performed Multiparametric Magnetic Resonance Imaging Helps to Differentiate Common Subtypes of Renal Tumours. *Eur Radiol.* 2014 May;24(5):1068-1080.
- 27.Vargas HA, Chaim J, Lefkowitz RA, et al. Renal Cortical Tumors: Use of Multiphasic Contrast-Enhanced Mr Imaging to Differentiate Benign and Malignant Histologic Subtypes. *Radiology.* 2012 Sep;264(3):779-788.
- 28.Vendrami CL, Velichko YS, Miller FH, et al. Differentiation of Papillary Renal Cell Carcinoma Subtypes on Mri: Qualitative and Texture Analysis. *AJR Am J Roentgenol.* 2018 Dec;211(6):1234-1245.
- 29.Goyal A, Razik A, Kandasamy D, et al. Role of Mr Texture Analysis in Histological Subtyping and Grading of Renal Cell Carcinoma: A Preliminary Study. *Abdom Radiol (NY).* 2019 Oct;44(10):3336-3349.